

amide. This led to 0.83 g of **6**. The NMR characterization was as for **1**, which indicates that no substantial substitution occurred.

Received: January 15, 2001  
Final version: June 6, 2001

- [1] a) J. M. J. Fréchet, *Science* **1994**, 263, 1710. b) V. Percec, C.-H. Ahn, G. Ungar, D. J. P. Yearley, M. Möller, S. S. Sheiko, *Nature* **1998**, 391, 161. c) A. Archut, F. Vögtle, *Chem. Soc. Rev.* **1998**, 27, 233. d) Y. H. Kim, *J. Polym. Sci., Part A: Polym. Chem.* **1998**, 36, 1685. e) H. Frey, C. Lach, K. Lorentz, *Adv. Mater.* **1998**, 10, 279. f) G. R. Newkome, E. He, C. N. Moorefield, *Chem. Rev.* **1998**, 99, 1689. g) M. Fischer, F. Vögtle, *Angew. Chem. Int. Ed.* **1999**, 38, 884.
- [2] C. J. Hawker, E. E. Malmström, C. W. Frank, J. P. Kampf, *J. Am. Chem. Soc.* **1997**, 119, 9903.
- [3] L. Eldada, L. W. Shacklette, *IEEE J. Select. Top. Quantum Electron.* **2000**, 6, 54.
- [4] M. Usui, M. Hikita, T. Watanabe, M. Amano, S. Sugawara, S. Hayashida, S. Imamura, *J. Lightwave Technol.* **1996**, 14, 2338.
- [5] C. Pitois, D. Wiesmann, S. Vukmirovic, M. Robertsson, A. Hult, *Macromolecules* **1999**, 32, 2903.
- [6] C. Roscher, R. Buestrich, P. Dannberg, O. Rosch, M. Popall, in *Proc. Organic/Inorganic Hybrid Materials Symposium of the 1998 MRS Spring Symposium*, San Francisco, CA, **1998**, p. 518.
- [7] M. B. J. Diemeer, T. Boonstra, M. C. J. M. Donckers, A. M. van Haperen, B. H. M. Hams, T. H. Hoekstra, J. W. Hofstraat, J. C. Lamers, W. Y. Mertens, R. Ramsamoedj, M. van Rheede, F. M. M. Suijten, U. E. Wiersum, R. H. Woudenberg, *Proc. SPIE* **1995**, 2527, 411.
- [8] T. M. Miller, T. X. Neeman, E. W. Kwock, S. M. Stein, *J. Am. Chem. Soc.* **1993**, 115, 356.
- [9] T. M. Miller, T. X. Neeman, R. Zayas, H. E. Bair, *J. Am. Chem. Soc.* **1992**, 114, 1018.
- [10] C. J. Hawker, R. Lee, J. M. J. Fréchet, *J. Am. Chem. Soc.* **1991**, 113, 4583.
- [11] J. Burdon, W. T. Westwood, *J. Chem. Soc. C* **1970**, 1271.
- [12] W. J. Dale, H. E. Hennis, *J. Am. Chem. Soc.* **1958**, 80, 3645.
- [13] a) N. Kanoh, A. Gotoh, T. Higashimura, S. Okamura, *Makromol. Chem.* **1963**, 63, 115. b) J. Ericsson, A. Hult, *Polym. Bull.* **1987**, 18, 295.
- [14] Commercially available mixture of aryl sulfonium hexafluoroantimonates (UVI 6974 from Union Carbide).
- [15] M. Lindgren, J. Örtengren, P. Busson, A. Eriksson, D. S. Hermann, A. Hult, U. W. Gedde, P. Rudquist, S. T. Lagerwall, B. Stebler, *Proc. SPIE* **1998**, 3475, 76.
- [16] A. Skumanich, J. C. Scott, *Mol. Cryst. Liq. Cryst.* **1990**, 183, 365.
- [17] J. F. W. McOmie, M. L. Watts, D. E. West, *Tetrahedron* **1968**, 24, 2289.

## Superconducting MgB<sub>2</sub> Nanowires\*\*

By Yiyang Wu, Benjamin Messer, and Peidong Yang\*

The recent discovery of superconducting MgB<sub>2</sub> with transition temperature ( $T_C$ ) of 39 K has stimulated great interest.<sup>[1–6]</sup> With its remarkably high  $T_C$  and the strongly coupled nature of the grain boundaries, MgB<sub>2</sub> is a promising material for practical application in superconducting devices. Many groups have put efforts in preparing superconducting MgB<sub>2</sub> thin films<sup>[4]</sup> and wires.<sup>[5,6]</sup> Until now, there is no report on the preparation of MgB<sub>2</sub> nanowires. It is fundamentally interesting to study the effect of dimensionality and size on superconductivity using MgB<sub>2</sub>

nanowire as model system.<sup>[7,8]</sup> In addition, MgB<sub>2</sub> nanowires can also serve as the building blocks in superconducting nanodevices such as low dissipation interconnects. Here we report the first preparation of MgB<sub>2</sub> nanowires by a two-step vapor transport and reaction process. In the first step, boron nanowires are prepared by chemical vapor transportation reaction. These boron nanowires are then transformed into MgB<sub>2</sub> nanowires by reacting with Mg vapor. The as-prepared nanowires have diameters of 50–400 nm and length up to tens of micrometers.

The preparation of boron nanowires was carried out in a sealed quartz tube. 20–35 mg boron, 0.5–1 mg I<sub>2</sub>, and 0.1–0.5 mg Si were put in one end of the tube (diameter 0.5 inch, length 3 inch, 1 inch ≈ 2.5 cm) and an MgO substrate was put in the other end of the tube. The MgO substrate was coated with 5 nm Au thin film using Desktop II Denton sputtering system. The tube was evacuated to 100 mtorr, sealed and then heated to 1000–1100 °C. A temperature gradient of 100 °C was kept between the source materials and the MgO substrate. At the hot zone, boron reacts with I<sub>2</sub> and forms BI<sub>3</sub> vapor. At low temperature zone, BI<sub>3</sub> vapor decomposes, as a result, boron deposits onto the MgO substrate. After 30 min of transport reaction, the furnace is cooled down to room temperature. Fluffy black products were observed on MgO substrate.

Figure 1a shows the scanning electron microscopy (SEM) image of the prepared boron nanowires. The whole substrate is covered with nanowires hundreds of micrometers long and 50–100 nm in diameter. Transmission electron microscopy (TEM) provides a closer look of the nanowires as shown in Figure 1b. Selected area electron diffraction (SAED) shows that these nanowires are amorphous and no diffraction spots or rings were observed. The elemental composition of these nanowires are analyzed by electron energy loss spectroscopy (EELS, Fig. 2c) and energy dispersive X-ray spectroscopy (EDX), which unambiguously show that the prepared nanowires are indeed boron nanowires slightly doped with Si. The inset of Figure 1b shows a TEM image of the tip of one boron nanowire. EDX analysis shows that this nanowire tip is composed of Au, Si, and boron. The presence of this Au/Si/B alloy droplet suggests the growth mechanism is the well-known vapor–liquid–solid (VLS) process<sup>[9–11]</sup> with Au as the liquid solvent at high temperature. In the current experiments, it's important to add small amount of Si into reactants. Contrast experiments where no Si was added in the system show essentially no nanowire growth on the substrate. We believe that the small amount of Si is critical for the easy formation of liquid alloy droplets on the substrate and the initiation of VLS nanowire growth. In fact, the eutectic temperature in B–Au binary phase diagram is as high as 1056 °C at 1 atm while it's only 363 °C for Si–Au system.<sup>[12]</sup>

The transformation of boron nanowires into MgB<sub>2</sub> nanowires is carried out in a sealed Ta tube by reacting with Mg vapor. The as-prepared boron nanowires and a Mg pellet were sealed into a Ta tube under Ar gas. Since MgB<sub>2</sub> is the Mg richest compound in Mg–B phase diagram, excess Mg was loaded in the tube. The Ta tube was further sealed in quartz tube and heated up to 800–900 °C for 2 h. The reaction ampoule was then removed from the furnace and quenched to room temperature.

[\*] Prof. P. Yang, Y. Wu, B. Messer  
Department of Chemistry, University of California  
Materials Science Division, Lawrence Berkeley National Laboratory  
Berkeley, CA 94720 (USA)  
E-mail: pyang@cchem.berkeley.edu

[\*\*] We thank the National Center for Electron Microscopy for the use of their facilities. P. Y. thanks the ACS-Petroleum Research Funds, Dreyfus foundation, 3M, Sloan Foundation, National Science Foundation, Department of Energy and University of California, Berkeley for support of this work. We thank Prof. J. Long and Mr. D. L. Beauvais for assistance with the boride transformation experiments.

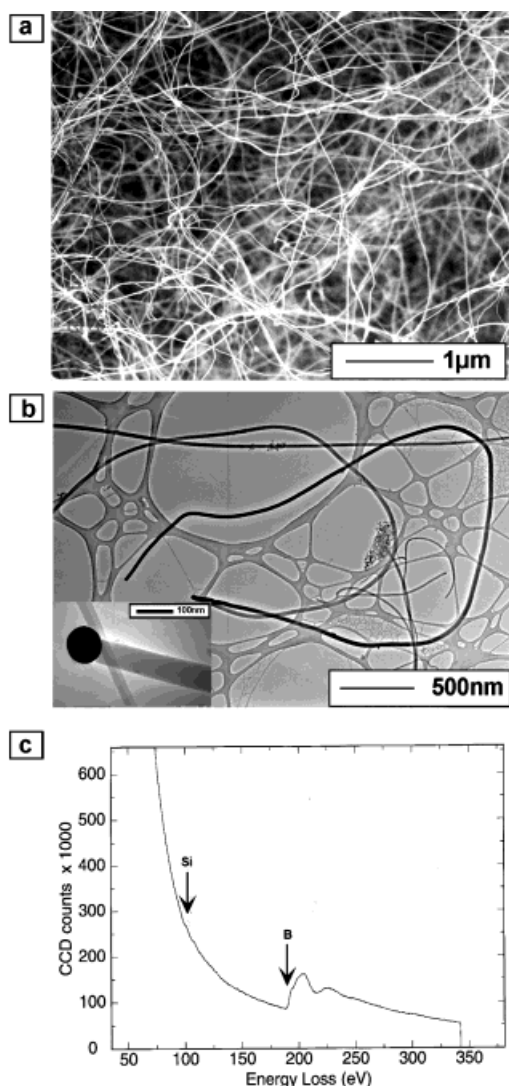


Fig. 1. a) SEM image of the boron nanowires. b) TEM image of the boron nanowires. The inset shows the tip of one nanowire. c) EELS spectrum recorded on the boron nanowires.

The transformed nanowires are thoroughly characterized by SEM, TEM, SAED, EELS, and EDX. Figure 2a shows a SEM image of the  $\text{MgB}_2$  nanowires on  $\text{MgO}$  substrate. The transformed nanowires are thicker than the original boron nanowires and the surface becomes rough. Before the transformation reaction, the boron nanowires are 50–100 nm in diameter. After the reaction, the diameter increases to 50–400 nm. TEM image (Fig. 2b) shows a closer look of these nanowires. SAED pattern (Fig. 2c) shows that the nanowires are polycrystalline. The diffraction pattern can be readily indexed as (100), (101), (110), (201) of the hexagonal  $\text{MgB}_2$  structure with  $a = 3.08 \text{ \AA}$  and  $c = 3.52 \text{ \AA}$ . Elemental analysis by EELS and EDX further confirmed the transformed nanowires are  $\text{MgB}_2$  nanowires slightly doped with Si.

Magnetization measurement on the as-prepared  $\text{MgB}_2$  nanowires was performed with a superconducting quantum interference device (SQUID) magnetometer (MPM2, Quan-

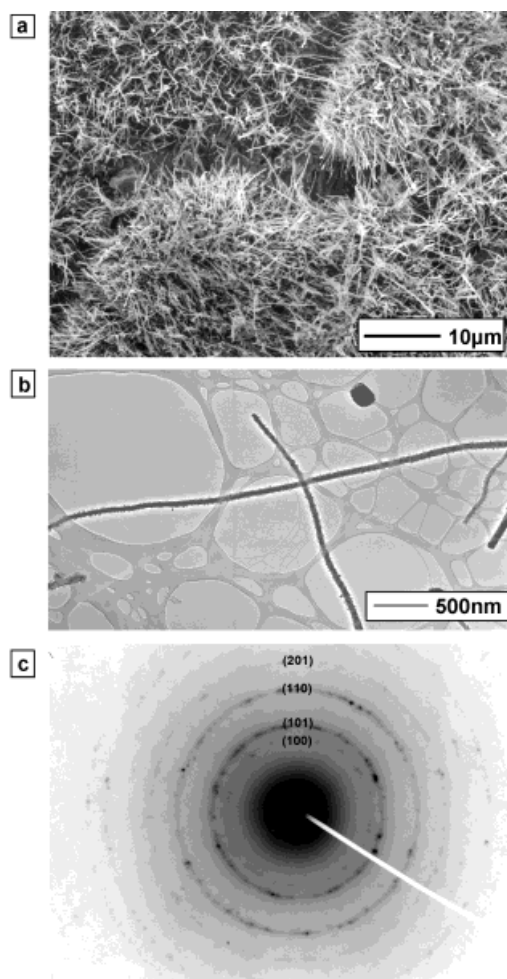


Fig. 2. a) SEM image of the  $\text{MgB}_2$  nanowires. b) TEM image of the  $\text{MgB}_2$  nanowires. c) SAED pattern recorded on the  $\text{MgB}_2$  nanowires. The diffraction rings are indexed according to the bulk  $\text{MgB}_2$  crystal structure.

tum Design). The magnetization as a function of temperature is shown in Figure 3, under condition of zero field cooling (ZFC) and field cooling (FC) in 100 G field. The existence of superconductivity within the sample is confirmed with the strong Meissner effect at  $\sim 33 \text{ K}$ .

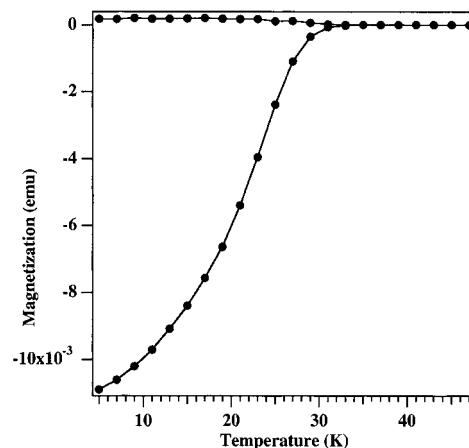


Fig. 3. Magnetization of  $\text{MgB}_2$  nanowires as a function of temperature. Data are shown for measurements under conditions of ZFC and FC at 100 G.

In summary, MgB<sub>2</sub> nanowires with diameter of 50–400 nm are prepared by reacting boron nanowires with Mg vapor. The superconductivity of these nanowires is confirmed by magnetization measurement. These superconducting nanowires can be potentially used as the building blocks in superconducting nanodevices and as low dissipation interconnects in nanoscale electronics.

Received: June 25, 2001

- [1] J. Nagamatsu, N. Nakagawa, T. Muranaka, Y. Zenitani, J. Akimitsu, *Nature* **2001**, *410*, 63.
- [2] D. C. Larbalestier, L. D. Cooley, M. O. Rikel, A. A. Polyanskiy, J. Jiang, S. Patnalk, X. Y. Cai, D. M. Feldmann, A. Gurevich, A. A. Squitieri, M. T. Naus, C. B. Eom, E. E. Hellstrom, R. J. Cava, K. A. Regan, N. Rogado, M. A. Hayward, T. He, J. S. Slusky, P. Khalifah, K. Inumaru, M. Hass, *Nature* **2001**, *410*, 186.
- [3] D. G. Hinks, H. Claus, J. D. Jorgensen, *Nature* **2001**, *411*, 457.
- [4] W. N. Kang, H. J. Kim, E. M. Choi, C. U. Jung, S. I. Lee, *Science* **2001**, *292*, 1521.
- [5] P. C. Canfield, D. F. Finnermore, S. L. Bud'ko, J. E. Ostenson, G. Laperot, C. E. Cunningham, C. Petrovic, *Phys. Rev. Lett.* **2001**, *86*, 2423.
- [6] S. Jin, H. Mavoori, C. Bower, R. B. van Dover, *Nature* **2001**, *411*, 563.
- [7] M. Tinkham, *J. Supercond.* **2000**, *13*, 801.
- [8] A. Bezryadin, C. N. Lau, M. Tinkham, *Nature* **2000**, *404*, 971.
- [9] R. S. Wagner, in *Whisker Technology* (Ed: A. P. Levitt), Wiley, New York **1976**, pp. 46–119.
- [10] Y. Wu, P. Yang, *J. Am. Chem. Soc.* **2001**, *123*, 3165.
- [11] A. Morales, C. M. Lieber, *Science* **1998**, *279*, 208.
- [12] *Binary Alloy Phase Diagram* (Ed: T. B. Massalaski), ASM Int., Materials Park, OH **1990**.

## Bicrystalline Silicon Nanowires\*\*

By Altaf H. Carim,\* Kok-Keong Lew, and Joan M. Redwing\*

A remarkable range of near-one-dimensional nanostructures can now be synthesized, including carbon nanotubes,<sup>[1]</sup> oxide nanobelts (ribbons),<sup>[2]</sup> and nanowires of metals,<sup>[3]</sup> oxides,<sup>[4]</sup> and semiconductors.<sup>[5,6]</sup> These offer many opportunities for basic understanding of the behavior of matter in restricted geometries<sup>[7]</sup> and suggest new electronic device structures with dimensions smaller than those available by traditional lithographic methods.<sup>[8]</sup> Silicon nanowires have been a subject of particular attention; they can be grown in single crystal form,<sup>[5,9,10]</sup> achieve high aspect ratios,<sup>[7,11]</sup> and exhibit quantum confinement effects at sufficiently small diameters.<sup>[12–14]</sup> Here we demonstrate the synthesis of bicrystalline silicon nanowires containing a single (111) twin boundary along the entire length of the [112] growth axis. The wires are generally straight and contain no other defects (twins, stacking faults, etc.). These unusual structures offer model systems for the

study of charge and mass transport along single defects and could serve as templates for novel device structures.

The materials discussed here were grown by a method combining vapor–liquid–solid (VLS) growth with the use of an anodic alumina membrane as an initial template.<sup>[15]</sup> Electrodeposition was used to position gold particles within the pores of the membrane (200 nm nominal pore diameter), approximately 10–30 μm from the top surface of the pores. The VLS growth was then carried out at 500 °C using a 5 % mixture of SiH<sub>4</sub> in H<sub>2</sub>. The gold particles nucleated and catalyzed the growth of Si nanowires within the membrane, which continued even after the nanowires reached the top surface and emerged from the pores. Wires protruding from the top of the membrane were then physically scraped off and dry dispersed onto a lacey carbon film supported by a 3 mm copper grid for microscopic analysis. Transmission electron microscopy (TEM) was performed on a Hitachi HF2000 cold field emission instrument with a 200 kV accelerating voltage, a 0.24 nm point resolution limit, and a 0.15 nm information limit.

A low-magnification image containing several bicrystalline (singly-twinned) nanowires is shown in Figure 1a. The long, vertical wire near the center of the image is aligned with the beam perpendicular to the growth axis and parallel to the [110] zone axis. Minor variations in contrast along its length result from a slight bending of the wire, causing changes in transmitted and diffracted intensity. In this orientation, the

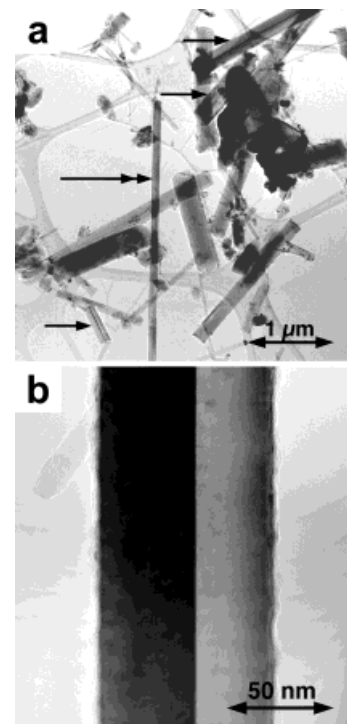


Fig. 1. Bright-field TEM images of bicrystalline silicon nanowires. a) Low-magnification image of nanowires supported on a lacey carbon film. The nanowire marked with a double arrow near the center has a diameter of about 83 nm and is >6 μm in length, and is bicrystalline with a single {111} twin boundary parallel to the long growth axis. A portion of this particular nanowire is shown at higher magnification in (b), in which the crystal has been slightly tilted to provide strong contrast between the twin variants. Three other nanowire segments within the field of view in (a) (arrowed) are clearly bicrystals as well.

[\*] Prof. A. H. Carim, K.-K. Lew, Prof. J. M. Redwing  
Department of Materials Science and Engineering and the Materials  
Research Institute, The Pennsylvania State University  
University Park, PA 16802 (USA)  
E-mail: carim@ems.psu.edu

\*\*] This work was supported by the Penn State Materials Research Institute and the NSF Materials Research Science and Engineering Center on Collective Phenomena in Restricted Geometries. TEM work was performed in the electron microscopy facility of the Materials Characterization Laboratory at Penn State University. We thank B. R. Martin, T. E. Mallouk, and C. Reuther for assistance with electrodeposition and use of facilities.